AN INVESTIGATION OF VERTICAL EXTRAPOLATION OF THE VECTOR HORIZONTAL WIND FIELD

BURFORD A. CARLSON

AN INVESTIGATION OF VERTICAL EXTRAPOLATION OF THE VECTOR HORIZONTAL WIND FIELD

****

Burford A. Carlson

AN INVESTIGATION OF VERTICAL EXTRAPOLATION OF THE VECTOR HORIZONTAL WIND FIELD

by

Burford A. Carlson
Lieutenant, United States Navy

Submitted in partial fulfillment of
the requirements for the degree of

MASTER OF SCIENCE
IN
METEOROLOGY

United States Naval Postgraduate School
Monterey, California

1960

1960
Carlson, B.

AN INVESTIGATION OF VERTICAL EXTRAPOLATION OF THE VECTOR HORIZONTAL WIND FIELD

By

Burford A. Carlson

This work is accepted as fulfilling

the thesis requirements for the degree of

MASTER OF SCIENCE

IN

METEOROLOGY

from the

United States Naval Postgraduate School

ABSTRACT

Extrapolation techniques including the geostrophic and gradient thermal wind, average wind shear from United States Weather Bureau maximum-wind analyses, and persistence were statistically compared for January 1960 over the United States. Calculations were made for layers contained between 200 mb and 40,000 or 45,000 feet, the thicknesses averaging 2100 or 6500 feet, respectively. Graphic results are presented for both speed and direction errors for each type of extrapolation.

It is shown that low wind speed, cross-isobar flow, and large curvature are associated with significant extrapolation errors.

The author is grateful for the patience and expert counsel of Professor R. J. Renard of the United States Naval Postgraduate School, Monterey, California.

TABLE OF CONTENTS

LIST OF ILLUSTRATIONS

TABLE OF SYMBOLS AND ABBREVIATIONS

$\bar{\ }$	Bar indicates average of value for layer
$\underline{\ }$	Underline indicates vector
V_k	Actual wind at level k
$\triangle V$	Actual wind change through layer
Vgs	Geostrophic wind
$\triangle$ Vgs	Geostrophic thermal wind
Vg	Scaler magnitude of $\underline{V_K} + \underline{\triangle V_{gs}}$
Vgr	Gradient wind
$\triangle$ Vgr	Gradient thermal wind
Vr	Scaler magnitude of $\underline{V_k} + \underline{\triangle V_{gr}}$
$\triangle$ Vs	Change in wind speed through a layer, computed from shear chart (herein designated as "shear wind")
V_c	General term for resultant extrapolated wind, however computed
V_t	A fictitious wind obtained by applying a geostrophic wind scale ($\triangle$ z interval 200 feet) to isotherms at 5°C interval
T	Temperature
Tv	Virtual temperature
p	Pressure
z	Altitude above sea level
c	Speed of movement of a pressure system
d	Distance over which horizontal temperature gradient is measured
β	Angle between $\underline{V_k}$ and $\underline{Vgs}$ (plus for cross contour flow toward low pressure)
ψ	Angle between $\underline{V_k}$ and $\underline{c}$
f	Coriolis parameter

K_s	Streamline curvature
K_h	Trajectory curvature
g	Gravity
R_d	Gas constant for dry air
$\underline{t}, \underline{n}, \underline{k}$	Unit vectors for horizontal spherical flow
LMW	Level of maximum wind
α	Specific volume of air
$\frac{\partial p}{\partial s}$	Horizontal pressure gradient in the direction of flow ($\underline{t}$)
$\frac{\partial p}{\partial n}$	Total horizontal pressure gradient
$\dot{v}$	Tangential acceleration

1. Introduction

The progress of jet aircraft to higher and higher operating altitudes has created a demand for more precise upper-atmosphere information. At present, there is a particular need for an accurate description of the wind field in and about the tropopause. The meteorological parameters of most concern to aircraft operating at these high altitudes are the enroute winds and clear air turbulence. The former is normally obtained from soundings or other types of direct wind (or pressure) observations.

Actual upper level wind reports are frequently missing for such areas as oceans, unpopulated continental sectors, or enemy held territory in wartime. This deficiency may be corrected by vertical extrapolation of wind from a level of known data by employing various aids such as the horizontal temperature field, empirical values of the wind shear, or layer of maximum wind analyses, to name a few. Although each of these parameters have been studied individually by others, no comprehensive comparison of vertical extrapolations of the horizontal wind at high altitudes has been published.

This shortcoming prompted a comparative analysis of the following vertical extrapolation techniques in the vicinity of the tropopause: geostrophic thermal wind, gradient thermal wind, average vertical shear of the actual wind, and persistence.

2. Previous extrapolation studies

Various methods are presently employed to determine the horizontal wind field above the highest reported wind. The simplest extrapolation procedure considers the wind vector to remain constant with height. This is the best technique to use for short vertical distances (500 feet) or in areas where little change in the wind vector with height is indicated. Determination of the latter areas is dependent upon an accurate subjective analysis of the wind field below the desired level, on the dynamics of the wind field as associated with the temperature field and the location of the jet axis. The condition of $\Delta V/\Delta z = 0$ is least likely to be met a few thousand feet above and below the tropopause and level of maximum wind.

The geostrophic thermal wind is often used for extrapolation through layers in which the wind field is changing rapidly. This method requires the determination of the mean horizontal temperature field for the layer. Lacking a mean temperature field, the isotherms at some level within the layer are often substituted for that of the former.

A few synoptic studies of the geostrophic thermal wind have been made. In a recent survey by Cunningham [2] accurate wind and temperature data were obtained from a specially instrumented B-29 flying at 280 and 383 mb over the United States on tracks perpendicular to the jet stream. Percent departures of the geostrophic and gradient thermal wind

extrapolations from the observed shear decrease exponentially with increasing distance (d) over which the horizontal temperature gradient was measured. Results were only slightly better for the gradient computations. Cunningham considered the lack of a large difference between the two methods due to the small isobar curvatures in the sample (maximum curvature approximately 1/1000 nautical miles).

To illustrate the advantage of using a mean wind, Cunningham averaged the wind over d before vectorially adding the geostrophic thermal wind to obtain the upper level wind. The departure of this wind from the actual wind varied inversely with d, and decreased from 11 percent at 33 miles to 2.7 percent at 181 miles. Even better results (two percent improvement) were achieved when using a mean verification wind as averaged over d, rather than a spot wind.

In order to understand the wind distribution about the jet core and perhaps to subjectively adjust vertical wind shear extrapolations, a knowledge of the jet stream is essential. Several empirical investigations of vertical shear in the vicinity of the jet stream have been recently published. Endlich [3] has developed a model cross section through the jet stream for use as an aid to forecasters in filling in areas of missing data. It provides an average wind distribution in a plane perpendicular to the jet in terms of percent of the speed at the jet core.

In a report on the layer of maximum wind, Reiter [6] indicates that, among other things, there is a lack of systematic dependence of the vertical decay of the wind on the magnitude of the maximum wind. However, he does show percent vertical decay as a function of the horizontal distance from the jet core. A later United States Navy AROWA study [10] obtained jet stream vertical shears that showed an increase with jet core speed. The magnitude of vertical shears above the core were indicated to be as much as 30 percent greater than those below. However, a United States Air Force study [9] of winds over 100 knots indicates the maximum vertical shears to lie below the maximum wind level.

A particularly useful description of the jet streams over the Pacific Ocean is provided by Serebreny [8] who presents numerous rules of thumb from statistical studies of these jets. A more comprehensive theoretical presentation of jet stream information is provided by Riehl et al [7] .

3. Theoretical development

The equation of horizontal motion in natural coordinates can be written as [5]

$$-\dot{V}\underline{n} + (V K_h + f)\underline{V} = -\alpha \underline{\nabla}_p z \times \underline{k} \qquad (1)$$

This becomes the gradient wind equation for $\dot{V} = 0$, and as a special case, the geostrophic wind equation when, additionally, $K_h = 0$.

In a manner similar to the development by Forsythe [4], equation (1) is differentiated with respect to p to obtain

$$-\frac{\partial(\dot{V}\underline{n})}{\partial p} + (V K_h + f)\frac{\partial \underline{V}}{\partial p} + \underline{V}\left(\frac{\partial V K_h}{\partial p}\right) = -\frac{\partial\left(g \underline{\nabla}_p z \times \underline{k}\right)}{\partial p} \qquad (2)$$

Interchanging the $\underline{\nabla}_p$ and $\frac{\partial}{\partial t}$ operators, equation (2) becomes

$$-\frac{\partial(\dot{V}\underline{n})}{\partial p} + (V K_h + f)\frac{\partial \underline{V}}{\partial p} + \underline{V}\left(\frac{\partial V K_h}{\partial p}\right) = -g \underline{\nabla}_p \frac{\partial z}{\partial p} \times \underline{k} \qquad (3)$$

Substituting the hydrostatic equation ($\alpha \partial p = -g \partial z$) in equation (3) and dividing by α,

$$\frac{1}{g}\frac{\partial(\dot{V}\underline{n})}{\partial z} - \frac{1}{g}(V K_h + f)\frac{\partial \underline{V}}{\partial z} - \frac{1}{g}\underline{V}\left(\frac{\partial V K_h}{\partial z}\right) = \frac{\partial}{\alpha}\underline{\nabla}_p \frac{z}{z} \times \underline{k} \qquad (4)$$

Taking the logarithm of the equation of state ($p\alpha = R_d T_v$),

$$\ln p + \ln \alpha = \ln T_v + \ln R_d \qquad (5)$$

Applying the operator $\underline{\nabla}_p$ to equation (5) yields

$$\frac{1}{\alpha}\underline{\nabla}_p \alpha = \frac{1}{T_v}\underline{\nabla}_p T_v \qquad (6)$$

Substituting equation (6) in equation (4) and rearranging terms,

$$-\frac{\partial(\dot{V}\underline{n})}{\partial t} + \left(V\underline{t}_{z+1}\right)\frac{\partial \underline{V}}{\partial z} + \underline{V}\left(\frac{\partial V \underline{K}_h}{\partial t}\right) = \frac{-g}{T_v}\nabla_p T_v \wedge \underline{k} \qquad (7)$$

The tangential acceleration, $\dot{V}$, in the first term of (7) is equal to the component of the pressure force in the direction of the wind and is the most difficult to evaluate. The first term may be expanded by setting

$$\dot{V} = -\frac{\partial \underline{V}}{\partial t} = -\frac{\partial}{\partial t}(V \sin\beta) \qquad (8)$$

where β is the angle between the geostrophic and actual wind directions. Thus equation (7) becomes

$$-\frac{\partial(\dot{V}\underline{n})}{\partial t} = -f\frac{\partial V_g}{\partial z}(\sin\beta)\underline{n} - fV_g(\cos\beta)\frac{\partial \beta}{\partial t}\underline{n} - fV_g(\cos\beta)\frac{\partial z}{\partial t}\underline{n} \qquad (9)$$

Where large accelerations exist, β equals 20 to 30 degrees and $\frac{\partial \beta}{\partial z}$ is frequently three degrees per thousand feet and occasionally as high as nine degrees per thousand feet [4]. Studies by Riehl [7] have found β to be greater than ten degrees 50 percent of the time and greater than 20 degrees only 25 percent of the time in the vicinity of the jet stream, so that determination of β (much less $\frac{\partial \beta}{\partial z}$) from routine contour analysis is questionable. However, when values of β definitely greater than zero appeared, they were tabulated as an indication of large $\dot{V}$.

In this study, 200 mb has been selected as the known level. Little moisture exists at this height and the temperature averages approximately -55°C (218°K) over the United States for the period selected for study. The temperature field is assumed invariant from 200 mb to the extrapolated level with $\nabla_p \overline{T_v} = \nabla_p T$ (temperature measured at 200 mb). With the further assumption that K_h and $\dot{V}$ are identically zero, equation (7) becomes the geostrophic thermal wind equation

$$\frac{\partial \underline{V_{gs}}}{\partial s} = -\frac{g \nabla_p T \times \underline{k}}{f T} \qquad (10)$$

expressed in its scalar working form as

$$|\Delta V_{gs}| \sim \frac{1}{40} \frac{1000}{T} V_t \frac{\Delta z}{1000} \sim .11 V_t \frac{\Delta z}{1000} \qquad (11)$$

where V_t is obtained by applying a geostrophic wind scale for a contour interval of 200 feet, to isotherms at a 5°C interval.

The gradient thermal wind equation is determined from equation (7) by setting $\dot{V}$ equal to zero and using the above definition of the vector $\frac{\partial \underline{V_{gr}}}{\partial s}$. The equation is shown here in a finite difference form as a change through a layer Δz, where K_h is assumed constant.

$$\underline{\Delta V_{gr}} = \underline{\Delta V_{gs}} - \frac{\overline{\underline{V_{gr}}}\, K_h \underline{\Delta V_{gr}}}{f} - \frac{K_h \underline{\Delta V_{gr}}\, \overline{\underline{V_{gr}}}}{f} \qquad (12)$$

(A) (B) (C)

Equation (12) is expressed in this form for ease in handling the term containing the geostrophic thermal wind vector. Figures 1 and 2 illustrate schematic wind extrapolations using equations (10) and (12), respectively.

The horizontal trajectory curvature, K_h, is obtained from Blaton's equation

$$K_h = K_s \left(1 - \frac{c}{V} \cos\psi\right) \qquad (13)$$

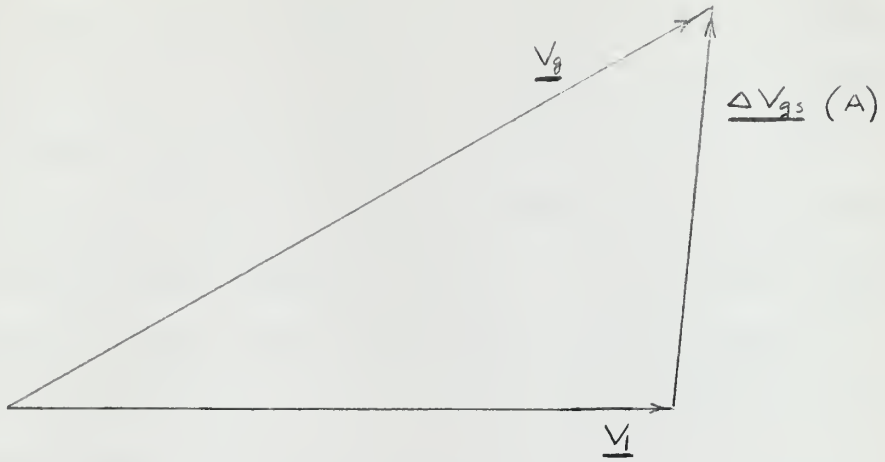

Figure 1. Schematic Geostrophic Thermal Wind Vector Diagram

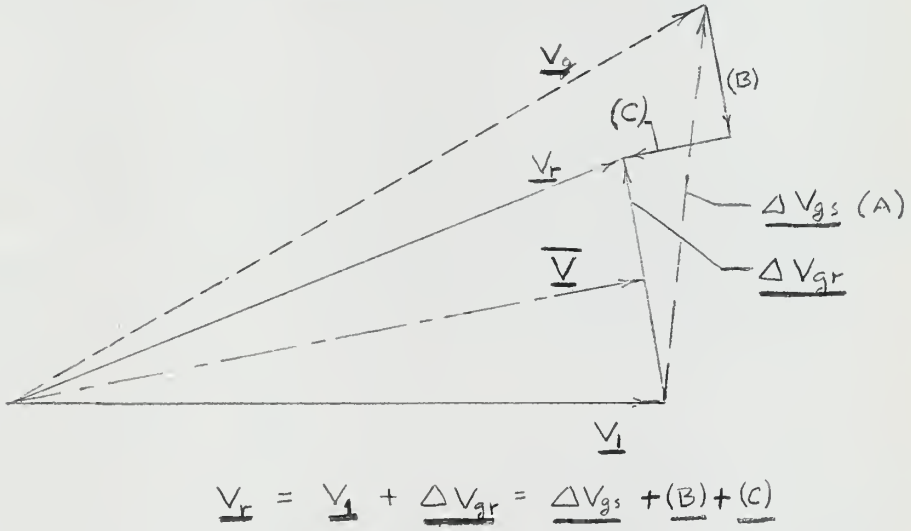

Figure 2. Schematic Gradient Thermal Wind Vector Diagram

4. Computation procedures

All data were obtained from 1200Z January 1960 United States Weather Bureau facsimile charts and concurrent upper wind reports. 200 mb was selected as the level of known data because, averaging 39,000 feet for this data sample, it was considered to be sufficiently close to both the level of maximum wind and the present jet aircraft maximum operating altitude. At each station extrapolations of winds to 40,000 and 45,000 feet were compared to reported winds at those levels. United States Weather Bureau tropopause-height and maximum-wind analyses for this period were also utilized.

a. Thermal wind extrapolations

Stations were chosen where a well defined thermal gradient existed from which the wind factor, $\underline{V_t}$, could be measured with a geostrophic wind scale as described in Section 3. $\underline{V_t}$ is multiplied by $.11\,\Delta z$ per thousand feet to obtain (A) in equation (12) and Figure 1. $\underline{V_1}$ is the vector wind at 200 mb. The wind at the upper level ($\underline{V_2}$) is obtained by the vector (graphical) addition of $\underline{\Delta V_{gs}}$ to $\underline{V_1}$.

For term (B), isobar curvature (K_s) is measured by the use of overlay arcs corrected for map scale variation. The 200-mb wind (V_1) and associated pressure-system movement (c) are determined and entered in equation (13) to yield trajectory curvature, K_h, considered constant through the layer.

The scalar $\overline{V_{gr}}$ is approximately equal to $\underline{V}$, the actual mean wind of the layer. As a first estimate of $\underline{\overline{V}}$, an

approximate vector mean of $\underline{V_g}$ and $\underline{V_1}$ may be obtained. An improvement is provided by the vector mean of $\underline{V_r}$ and $\underline{V_1}$.

Term (A), $\underline{\triangle Vgs}$, is used for the first estimate of $\underline{\triangle Vgr}$. The coriolis parameter (f) is taken from published tables [1]. Although (B) is a vector parallel to $\underline{\triangle Vgr}$, it may be drawn parallel to $\underline{\triangle Vgs}$ as a first approximation.

In term (C) $\triangle Vgr$ is initially considered equal to the scalar magnitude of $\underline{\triangle Vgs}$. Vector (C) parallels $\underline{\overline{Vgr}}$, approximately by $\underline{\overline{V}}$, which may be obtained as previously described or by trial and error.

The resultant $\underline{\triangle Vgr}$ is reentered in (B) and (C), $\underline{\overline{Vgr}}$ is recomputed and a second approximation to $\underline{\triangle Vgr}$ calculated. This is generally sufficient to produce the desired accuracy in $\underline{\triangle Vgr}$.

b. Shear-wind extrapolations

Over the United States, the facsimile maximum-wind analyses provide the height and velocity of the maximum wind and the vertical wind shear in the layer containing the level of maximum wind. (This level is hereafter referred to as the LMW). These shears are a subjectively determined average of the plotted shears 10,000 feet above and below the LMW.

The shear obtained from the chart is multiplied by the thickness of the extrapolation layer (in thousands of feet). This gives $\triangle Vs$ which is added to or subtracted from the wind at the known level (200 mb), depending upon whether it is below or above the LMW. For extrapolations crossing the LMW, a net $\triangle Vs$

is obtained from the difference between ΔVs from 200 mb to the LMW and ΔVs from the LMW to the desired upper level. The wind direction is considered to remain constant through the layer.

A shear-wind computation was made for all stations for which a thermal wind computation was made.

5. Graphic analysis of computations

The objective of this study was to statistically consider the error distribution of various methods of vertical extrapolation of the horizontal wind field and its relation to other parameters, and thus determine the most accurate extrapolation procedure. A graphic representation was selected as best meeting these requirements.

a. Error discussion

Error as used herein is defined as:

(1) the angle between the extrapolated wind direction and the actual wind direction (from teletype reports) at a given level. A plus error means that the extrapolated wind had turned through a greater angle (and in the same direction) than the actual wind for the given layer, the bottom of which is at 200 mb. A minus error represents too little turning (or turning in the wrong direction) of the extrapolated wind. Therefore, for extrapolations using persistence, all errors are minus. However, since the distributions of the thermal-wind-direction extrapolations are nearly normal, a clearer comparison is obtained by distributing the persistence extrapolation errors symmetrically about an error of zero, i. e. for any given error, half the cases are considered plus, half are taken as minus.

(2) the difference between the extrapolated wind speed and the actual wind speed (from teletype reports) divided by the actual wind speed at the level. Thus, the result is expressed in percent of the actual wind speed.

It must be realized that, at times, extreme errors may arise solely due to errors in observing and reporting the winds. Reiter [6] has shown how the method of determining upper winds can produce the unrealistic oscillations sometimes found in vertical wind profiles. He also described how the abbreviated teletype codes can remarkably alter the actual upper-level sounding curve. His illustrations particularly emphasize the desirability of averaging and smoothing to obtain representative wind profiles.

Another error arises when the neglected term, the tangential acceleration becomes large. Subject to errors in analysis, cross-isobar flow is an indication that this acceleration is significant. To determine the effect of this term, the number of clearly apparent cross-isobar angles greater than 15 degrees have been recorded in boxes (☐) on the graphs which follow.

The number of winds under 20 knots have also been recorded in circles (◯) on the graphs. At this low wind speed, large errors in direction and percent speed result from small vector errors.

b. Data

Information from 150 soundings were utilized to obtain 107 layers whose thickness averaged 2100 feet (range from 900 to 3300 feet) and 149 layers whose thickness averaged 6500 feet (range from 3300 to 8400 feet). Two thermal wind extrapolations and a shear extrapolation were compared with persistence for each layer, considering direction and speed separately.

Of the 150 reports, 21 showed a near-zero thermal gradient at the 200-mb level, 45 had trajectories which were nearly straight (curvature less than 1/2500 nautical miles), 22 cases were associated with anticyclonic curvature, and 62 with cyclonic curvature.

The following factors were considered for their effect on the extrapolation error:

1. Cross-isobar angle
2. Location of the jet maximum in relation to the station (horizontal distance and direction)
3. Tropopause height
4. Level of maximum wind
5. Whether wind speed was increasing or decreasing with height
6. Angle between the thermal wind and actual wind
7. Magnitude of wind speed
8. Magnitude and algebraic sign of trajectory curvature
9. Magnitude of the thermal gradient

The graphs that follow represent the most significant results of the above considerations.

Figure 3.

This graph presents frequency of errors in the extrapolated angular turning of the wind for layers averaging 2100 feet. Little deviation from persistence is shown by the geostrophic or gradient thermal wind errors, since 87 percent of the geostrophic or gradient thermal wind computations lie within $\pm$ 15 degrees of the actual wind. Of the persistence cases,

84 percent fall within this range.

The slight skew toward negative angle error indicates that the computations, on the average, underestimate the actual angular turning. A further analysis of these winds indicates that this slight skewness is due to cases in which the wind speed decreases with increasing height.

Considering only the cases of $K_h > 1/2000$ nautical miles, where $\triangle$ Vgs exceeds two knots per thousand feet, does not change the substance of the foregoing conclusions.

As would be expected for extreme angular errors ($> |40$ degrees$|$), there are relatively large percentages of low-wind-speed, cross-isobar and large-curvature cases.

Figure 4

This figure presents the same type of information displayed in Figure 3, but only for extrapolations through layers averaging 6500 feet. For $\pm$ 15 degrees and $\pm$ 25 degrees errors, respectively, the included percentage frequencies are: 63 and 76 percent for persistence, 70 and 84 percent for geostrophic and 73 and 88 percent for gradient thermal wind extrapolations. The latter represents a significant improvement over persistence, although slighly skewed.

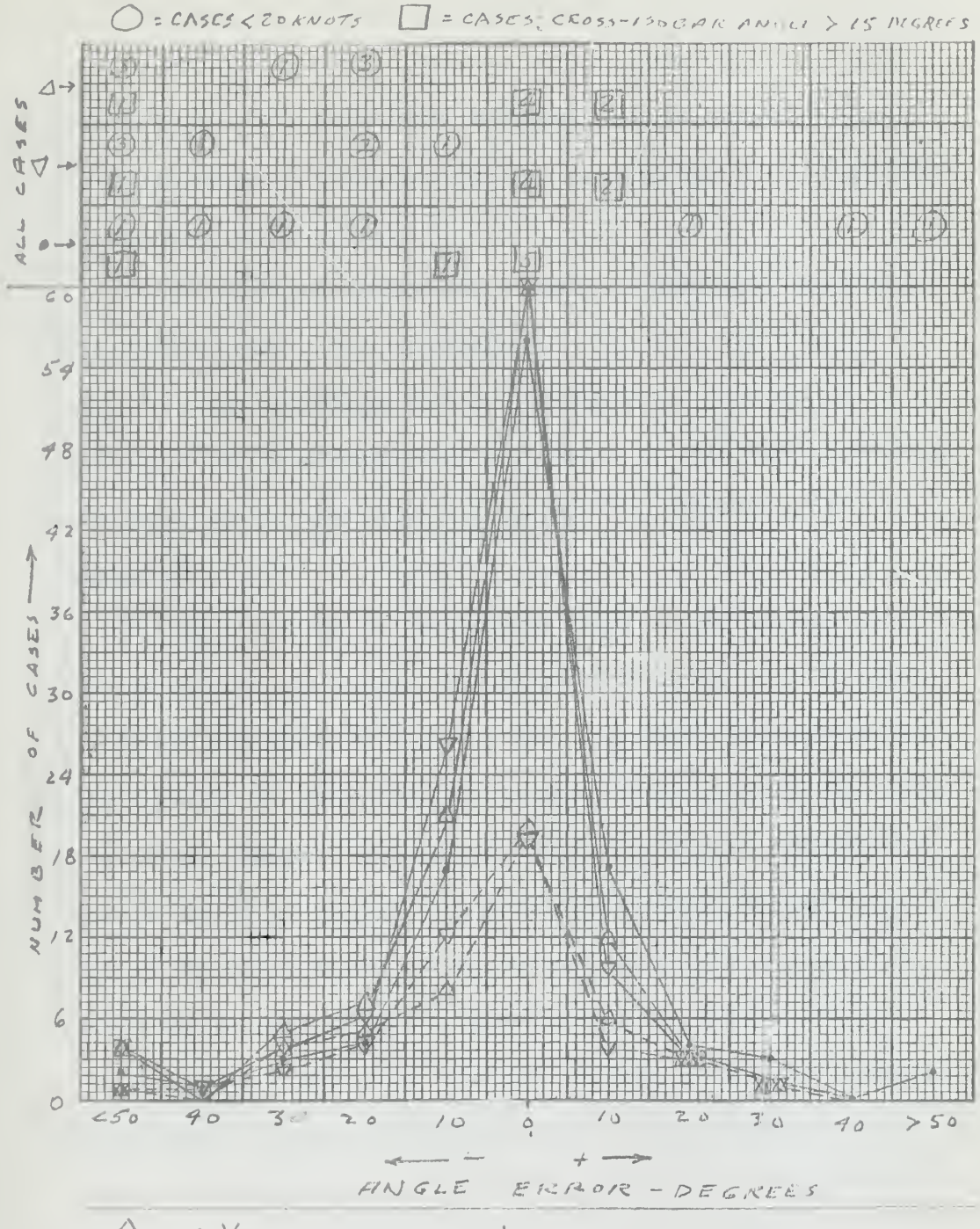

FIGURE 3. Frequency Distribution of Wind-Direction Errors (in degrees) - 2100 feet average thickness - all cases

The severest skewing is observed for the geostrophic cases, in contrast to figure 3. However, again, this effect is due to the cases of winds which show decrease with increasing height. At the extremes of the distribution, low wind speeds account for a large portion of the error.

Large curvature is present in most of the cases associated with errors greater than 20 degrees. Note that the mode for cases of large curvature lies at -10 degrees. Even so, 74 percent of the geostrophic and 82 percent of the gradient-thermal wind cases in this category lie within $\pm$ 25 degrees error.

Figure 5

The distribution of the percent error in the extrapolated wind speed from the actual (reported) wind speed is shown here, for layers averaging 2100 feet. All four types of computations peak together at zero with little skew except possibly the ΔV_s wind cases. Within $\pm$ 15 percent and $\pm$ 25 percent, respectively lies 66 and 80 percent of the persistence cases, 68 and 85 percent of the shear cases, 71 and 89 percent of the geostrophic and 75 and 90 percent of the gradient-thermal wind cases.

Persistence and shear show the maximum large error samples. As expected, they are associated with a correspondingly large number of cross-isobar and low-wind-speed cases. Cases with large curvature are considered on the next two graphs.

Figure 6

This figure depicts the error distributions for those extrapolations in figure 6 which are associated with winds

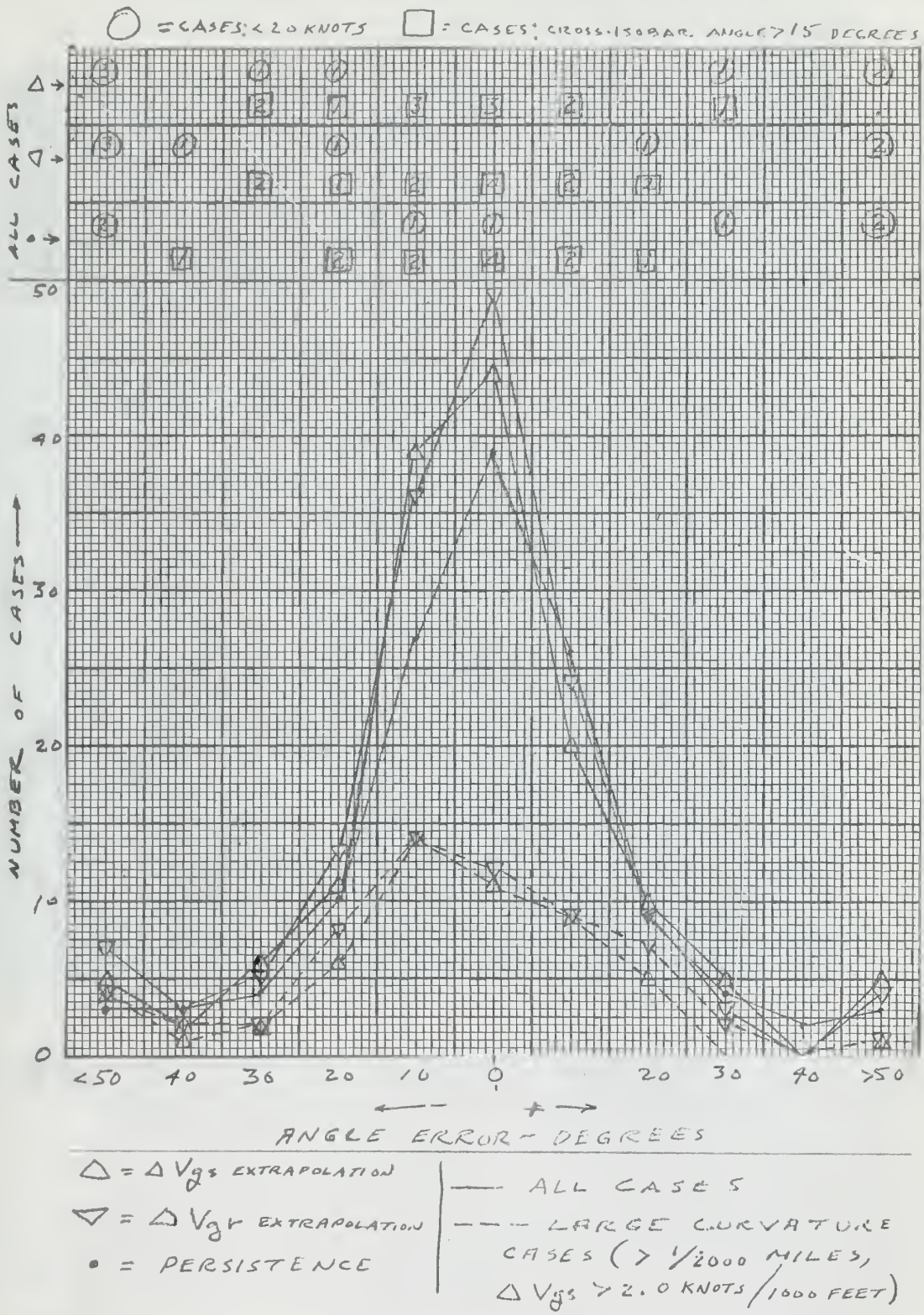

FIGURE 4. Frequency Distribution of Wind Direction Errors (in degrees) - 6500 feet average thickness - all cases

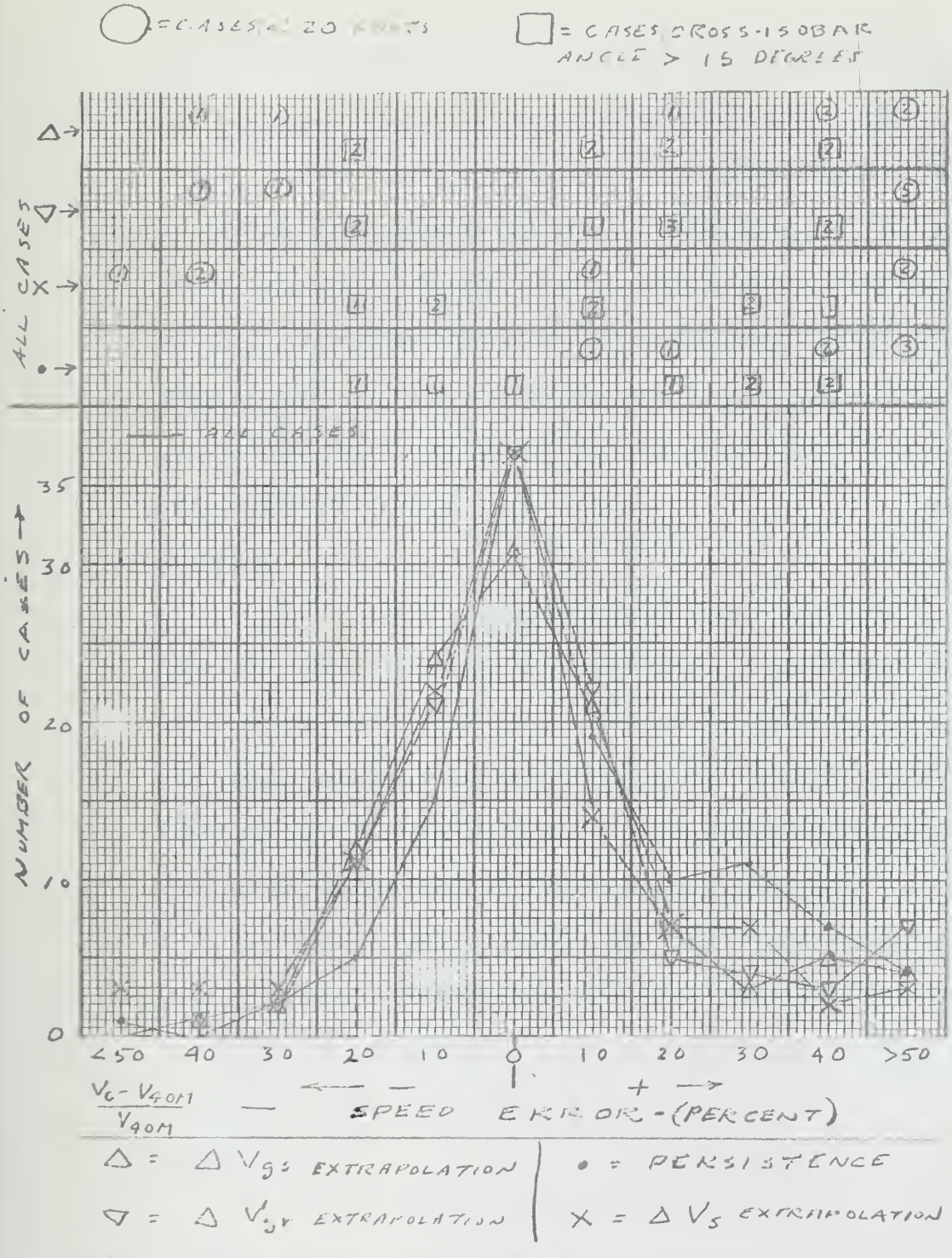

FIGURE 5. Frequency Distribution of Wind Speed Errors (in percent)
2100 feet average thickness - all cases

decreasing speed with increasing height. The curves in figures 5 and 6 are similar, except that persistence occurs only on the positive error side (because winds are decreasing). Figure 6 shows somewhat more irregularity than figure 5 because of the smaller sample in the former. Presuming the plus skew of the geostrophic thermal wind extrapolation curve is valid, it indicates the non-applicability of the simple geostrophic thermal wind for large curvature cases - a not unexpected result from theory in view of the high percentages of cyclonic cases considered here.

Figure 7

Figure 7 depicts the frequency of speed errors for cases of winds increasing with increasing height. Here is shown a pronounced skew, with a mode at -10 percent, for all techniques except persistence. The number of large curvature cases is again too small to be of great significance, although the curves follow those of figure 5 quite closely.

The overall skew indicates that none of the extrapolation techniques increases the wind speed adequately through the layer, the computations being on the average ten percent too low.

Figure 8

This picture indicates the extreme variability in the accuracy of wind speeds extrapolated through a layer averaging 6500 feet. Thermal wind computations show major peaks at both zero and -20 percent error so that a further error

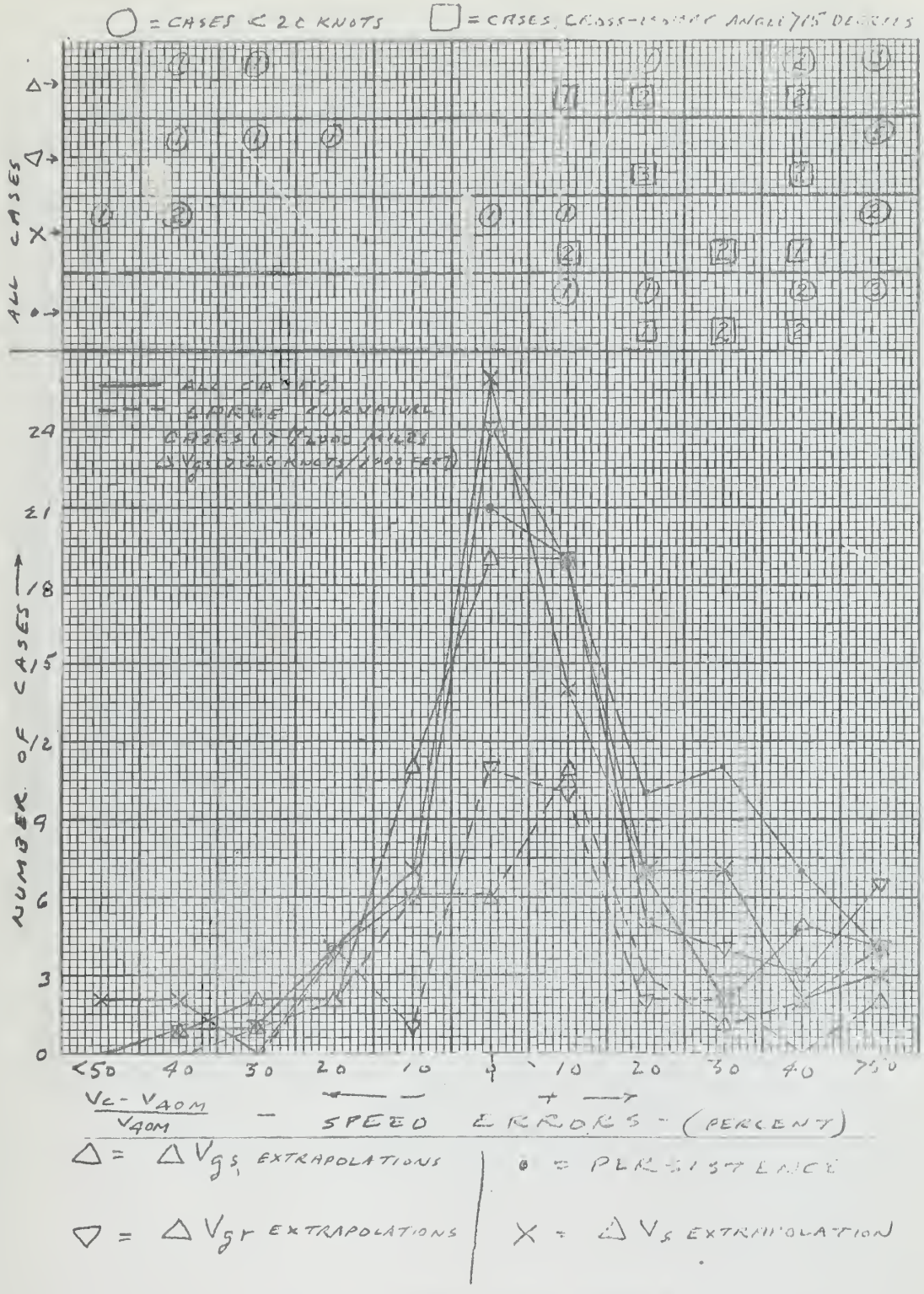

FIGURE 6. Frequency Distribution of Wind Speed Errors (in percent)

2100 feet average thickness - wind decreasing with height

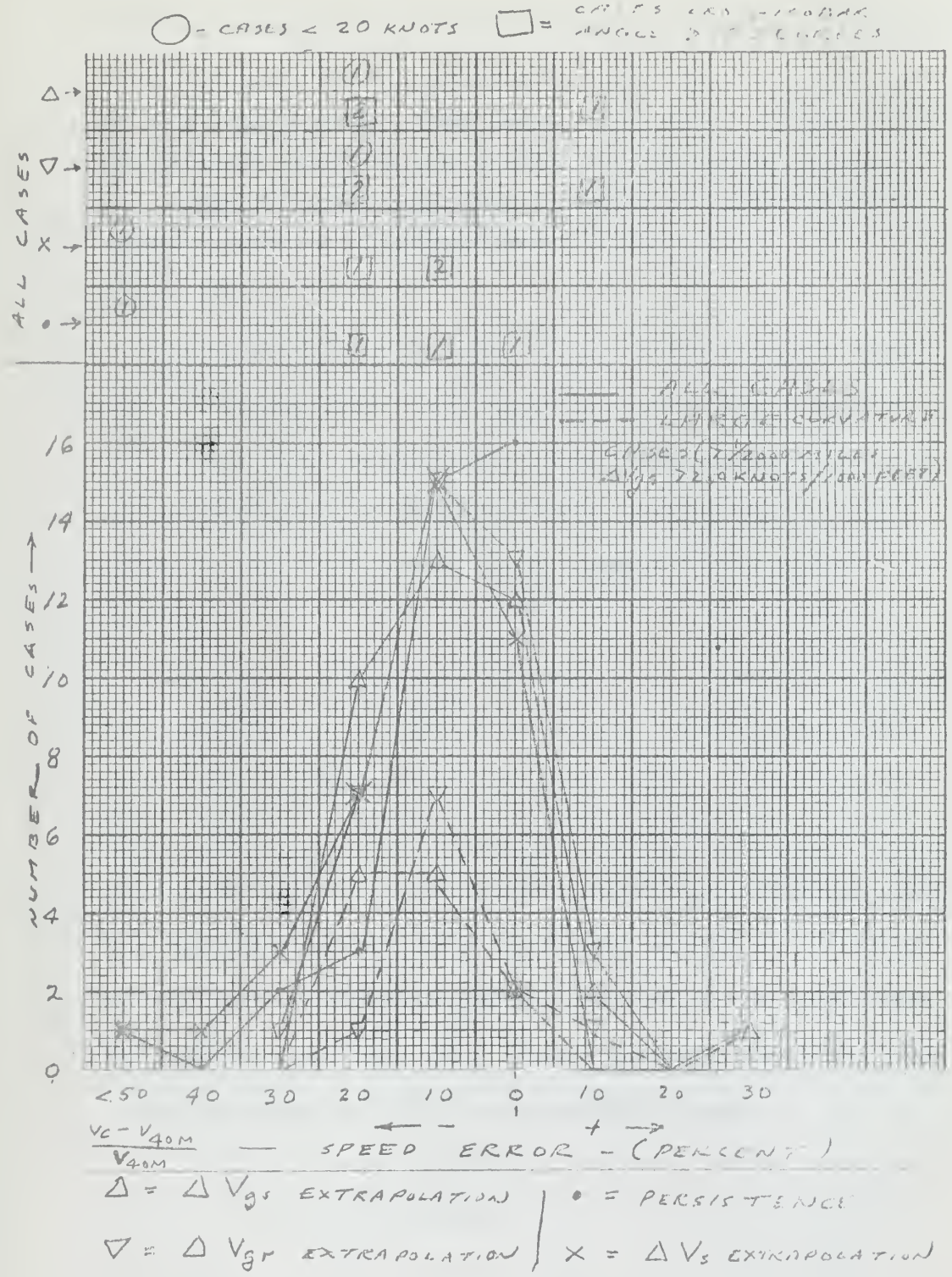

FIGURE 7. Frequency Distribution of Wind Speed Errors (in percent)

2100 feet average thickness - wind increasing with height

investigation was made necessary (figures 9 and 10). Persistence shows a broader curve, peaking at +10 percent and is apparently of less significance. Shear computations show a rather irregular distribution, with the mean approaching -20 percent error.

Large curvature cases have a mode at +10 percent with a secondary peak at -20 percent error.

Figure 9

Considering only the cases of wind which decreases speed with increasing height from figure 8, a much clearer mode at +10 percent error is obtained. These curves indicate that the computations either underestimate the decrease of wind with height or increase the wind on the average, by about ten percent.

The data for the secondary maximum at -20 percent error was examined, and in addition to several low-wind-speed and cross-isobar cases, there are four that cross the tropopause and six that pass through the layer of maximum wind. Some of the explanations for the occurrence of this type of error would be a secondary maximum above the primary maximum in the actual wind profile, an excessive thermal gradient at the level where the extrapolation began, or a thermal gradient associated with a relative minimum just above the original level.

The error curves indicate that the best results could be obtained by using persistence, if the wind was known to be decreasing. A wind at the top of the layer correct within $\pm$ 20 percent would be obtained 60 percent of the time by subtracting 15 percent from the wind at the known level. The

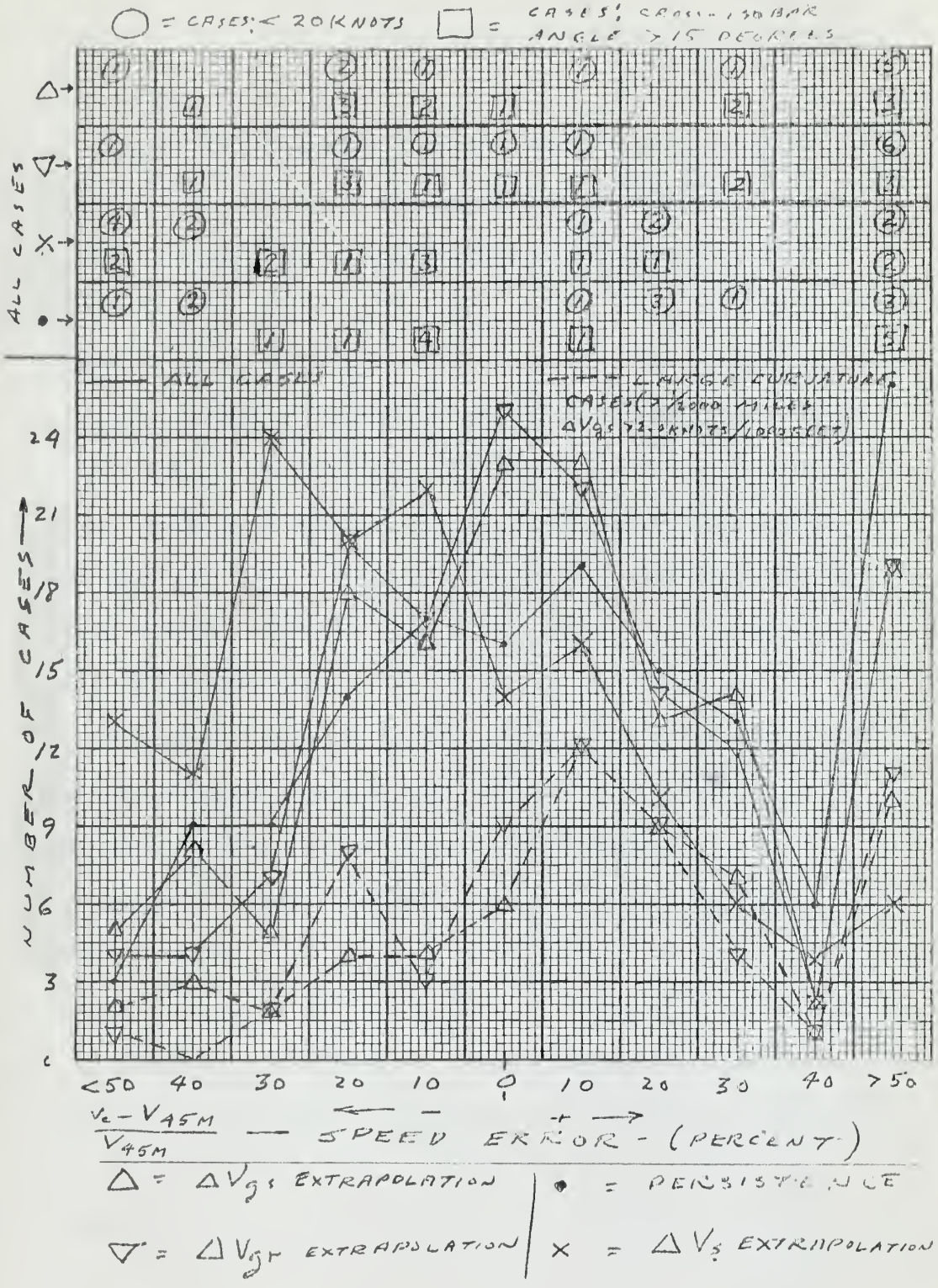

FIGURE 8. Frequency Distribution of Wind Speed Errors (in percent)

6500 feet average thickness - all cases

extreme errors (> 50 percent) that may arise, are in part attributable to the large number of cross-isobar and low-wind-speed cases there.

The curve for large curvature cases follows the parent curve in figure 8 except for the indication that here the geostrophic thermal wind extrapolations do not decrease the wind adequately.

Figure 10.

For the cases of winds increasing with increasing height in figure 8, shear extrapolations produce a maximum skew with a mode of -30 percent error. Both thermal wind computations have modes of zero, with 60 percent of the geostrophic and 66 percent of the gradient thermal wind computations lying in the range -5 ± 20 percent.

Persistence would be better, however, when the wind speed is known to be increasing, as 78 percent of the winds lie within $\pm$ 20 percent of a mean of -15 percent.

Large-curvature cases do not show any clear indications of relevant trends.

Table 1

The results in figures 5 - 10 indicate that it is important to know whether the winds are increasing or decreasing through a layer. Table 1 was assembled to predict the accuracy with which each extrapolation technique could give this information. Except for the shear computation through the thicker layer, the correct result can be expected 60 percent of the time.

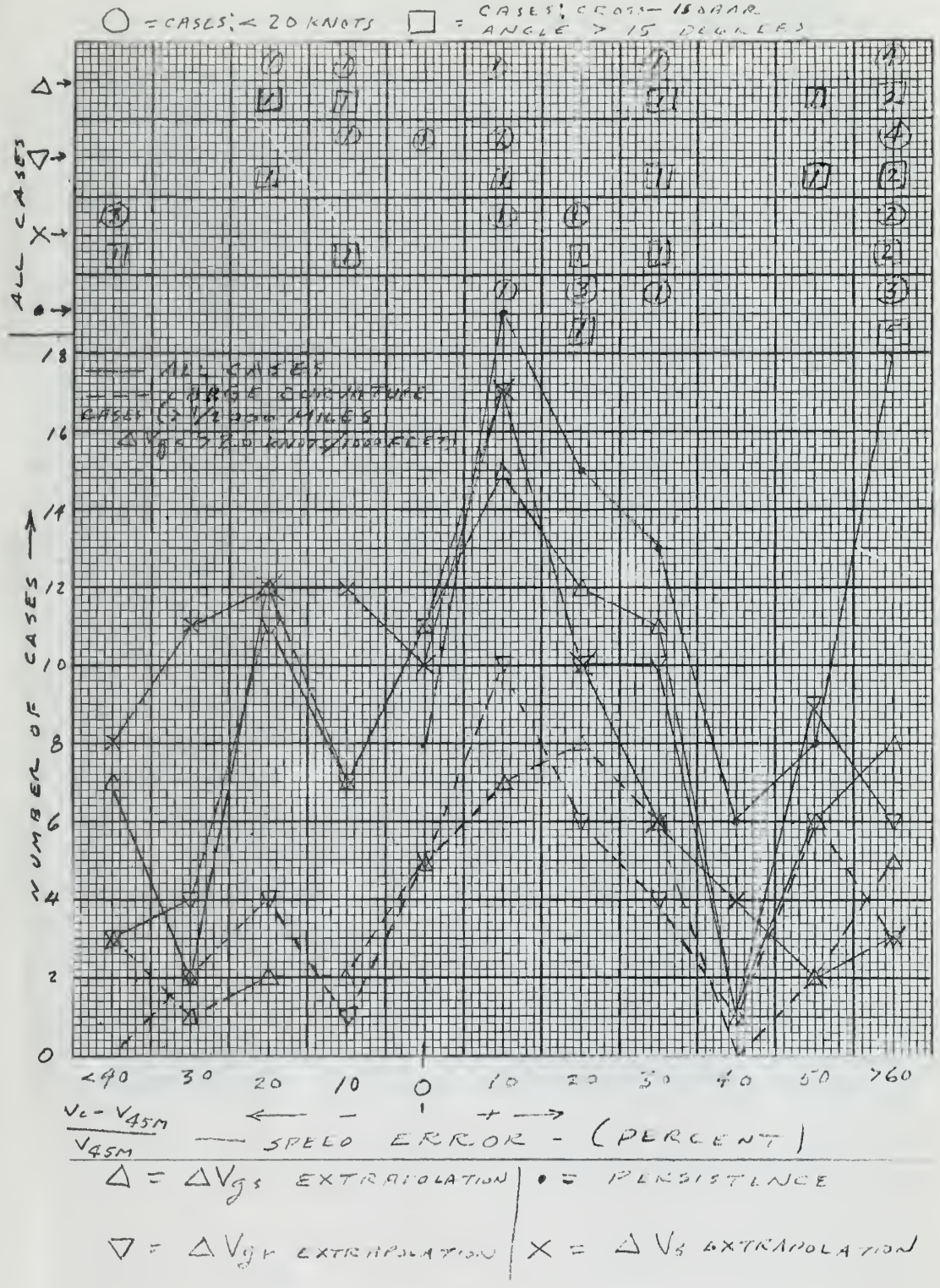

FIGURE 9. Frequency Distribution of Wind Speed Errors (in percent)

6500 feet average thickness - wind forecasting with height

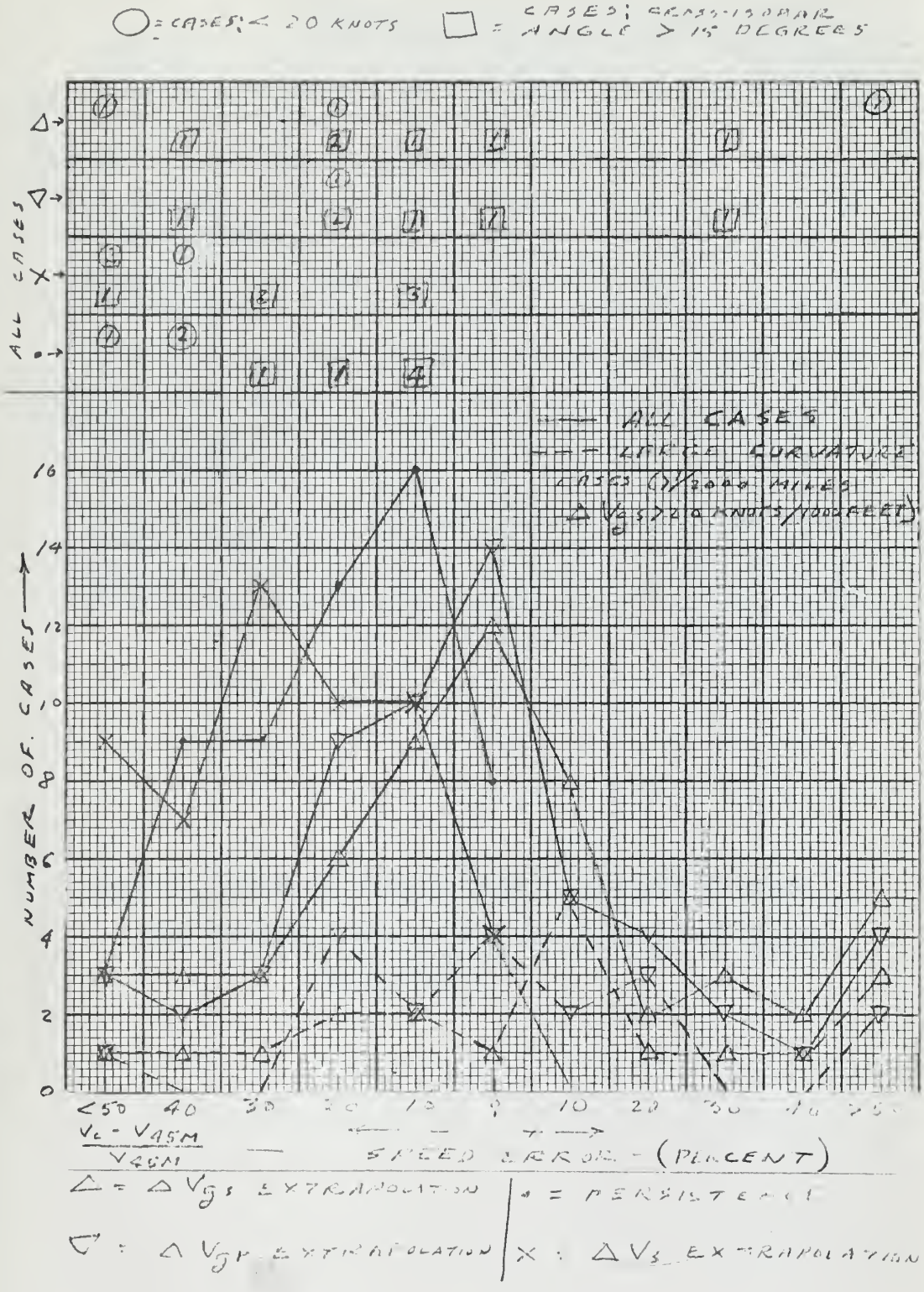

FIGURE 10. Frequency Distribution of Wind Speed Errors (in percent)

6500 feet average thickness - wind increasing with height

Δz / TYPE OF EXTRAPOLATION	ALGEBRAIC SIGN OF SPEED CHANGE CORRECT			ALGEBRAIC SIGN OF SPEED CHANGE INCORRECT		
	ΔV ≠ 0	ΔV = 0	TOTAL	ΔV ≠ 0	ΔV = 0	TOTAL
2100 Ft						
Geostrophic Thermal Wind	44	18	62	21	17	38
Gradient Thermal Wind	42	20	62	20	18	38
Shear	42	19	62	14	24	38
6500 Ft						
Geostrophic Thermal Wind	58	3	61	20	19	39
Gradient Thermal Wind	60	3	63	19	18	37
Shear	42	7	49	16	35	51

TABLE 1. Number of Cases (percent) of Correct Algebraic Sign of Speed Extrapolations as a Function of Type of Extrapolation

6. Conclusions

From this study, it is apparent that more accurate extrapolations in the vicinity of 200 mb can be made if the influence of various restrictive conditions is also considered. A qualitative estimate of the likelihood of encountering large errors is provided by the proportionately large number of cross-isobar and low-wind-speed (and possibly, large-curvature) cases occurring near the limits of the error distribution graphs. In addition, the type of extrapolation produces an intrinsic error. Even more important is the determination of whether the wind speed is increasing or decreasing with height.

Considering wind direction alone, for a 2100-foot layer, persistence is observed to be as good as either of the thermal wind extrapolations. For a 6500-foot layer the gradient thermal wind computation is superior, with 73 percent falling within $\pm$ 15 degrees and 88 percent within $\pm$ 25 degrees of actual turning through the layer. For large curvature cases in a 6500-foot layer, both thermal wind computations produce a small error that averages five degrees too little turning. Where computing time is limited, persistence, for these same cases, will produce an error less than 25 degrees 76 percent of the time.

Better results are obtained for vertical extrapolations of the speed using thermal wind extrapolations (thermal gradient accurate to $\pm$ 15 percent and $\pm$ 25 percent 75 and

90 percent of the time, respectively) compared to persistence or shear computations for a 2100-foot layer. For decreasing wind speed with height, geostrophic thermal wind computations do not decrease the wind sufficiently, whereas for increasing speed with height, all computations average ten percent low.

Extrapolation results for speed are least accurate for a 6500-foot layer. Generally, best results are obtained for shear computations with the speed error in the range -10 $\pm$ 25 percent, 70 percent of the time. For decreasing wind speed with increasing height, all curves peak near plus ten percent error with a secondary mode near -20 percent. Consequently, persistence minus 15 percent is correct within $\pm$ 20 percent of the true wind, 60 percent of the time. Even so, errors greater than 50 percent occur 20 percent of the time. Considering only increasing winds with height, thermal wind computations peak at zero. Again, persistence plus 15 percent yields 78 percent of the cases within $\pm$ 20 percent.

All thermal wind extrapolations predict the correct direction of shear(plus or minus) in the vicinity of 200 mb 60 percent of time as compared to 50 percent for shear-wind computations.

Other approaches that are recommended for further study, to obtain more accurate wind extrapolations, are listed below. (1) Instead of considering speed and direction separately, consider the magnitude (and perhaps direction) of the vector error (especially for low wind speeds).

(2) For a better comparison between geostrophic thermal wind and gradient thermal wind extrapolations, increase the number of large curvature cases.

(3) Study cross-isobar cases separately.

(4) Determine a more accurate method of predicting whether the wind is increasing or decreasing with increasing height.

(5) Separately determine the shear above and below the LMW and use for extrapolation studies.

BIBLIOGRAPHY

1. Berry, F. A. Bollay, E., Beers, N. R., Handbook of Meteorology, p. 116, McGraw Hill Book Co., Inc., 1945

2. Cunningham, N. W., A study of the thermal wind in the vicinity of a jet stream, 75th Anniversary Volume of the Journal of the Meteorological Society of Japan, Nov. 1957

3. Endlich, R. and McLean, G., Application of jet stream research to analysis and forecasting, A. F. Cambridge Res. Center, GRD-TM-57-9, 1957

4. Forsythe, Capt. G. E., A generalization of the thermal wind equation to arbitrary horizontal flow, Bull. Amer. Meteor. Soc., 9, pp. 371-375, Nov. 1945

5. Haltiner, G. J. and Martin, F. L., Dynamical and Physical Meteorology, chaps. 11-13, McGraw Hill Book Co,, Inc., 1957

6. Reiter, E., The layer of maximum wind, J. Meteor., Vol. 15, pp. 27-43, Feb. 1958

7. Riehl, H., Alaka, M. A., Jordan, C.L., Renard, R.J., The jet stream, Meteorological Monographs, Boston, Mass., Amer. Meteor. Soc., 2, No. 7, 1954

8. Serebreny, S. M., Wiegman, E.J., Carlson, W.F., Cronin,J.G., Forecasting manual for the jet stream over the Pacific, NAVAER 50-1P-536, PAA, San Francisco, Calif., 1955

9. _____, Air Weather Service Technical Report 105-21, Winds over 100 knots in the Northern Hemisphere, 1955

10. _____ _, AROWA, Jet stream probing, Task 15, U. S. Navy Research Facility, 1959.